Purdue University

Purdue e-Pubs

International Refrigeration and Air Conditioning Conference

School of Mechanical Engineering

2021

Correlation for Flow Boiling Heat Transfer of Low-pressure Refrigerants Inside A Horizontal Smooth Tube

Yufei Liu
Nagasaki University, liuyufei@nagasaki-u.ac.jp

Daisuke Jige
Tokyo University of Marine Science and Technology

Norihiro Inoue
Tokyo University of Marine Science and Technology

Correlation for Flow Boiling Heat Transfer of Low-pressure Refrigerants Inside A Horizontal Smooth Tube

Yufei LIU[1]*, Daisuke JIGE[2], Norihiro INOUE[2]

[1]Nagasaki University, Graduate School of Engineering,
Nagasaki, Japan
(+81-95-819-2504, liuyufei@nagasaki-u.ac.jp)

[2]Tokyo University of Marine Science and Technology,
Tokyo, Japan
(+81-3-5245-7479, djige00@kaiyodai.ac.jp, inoue@kaiyodai.ac.jp)

* Corresponding Author

ABSTRACT

The flow boiling heat transfer of low-pressure refrigerants including R1224yd(Z), R1233zd(E), R1336mzz(Z), and R1336mzz(E) was experimentally investigated inside a horizontal smooth tube with outer and inner diameters of 9.52 and 8.40 mm, respectively. The experiments were conducted at a mass velocity range of 50–300 $kgm^{-2}s^{-1}$ and a saturation temperature of 40 °C. In the forced convection region, where the vapor shear force was dominant, the measured heat transfer coefficients were slightly larger than those of the conventional refrigerants were. A modified heat transfer correlation was developed based on a wettability separation angle to differentiate the stratified and annular flows. In addition, the heat transfer coefficient after the onset of dryout vapor quality was studied. Within the entire database, the mean deviation of the modified correlation was 1.0 %. The developed correlation agreed better with the experimental results compared to the conventional correlations.

1. INTRODUCTION

A heat pump system that generates hot water and high-temperature steam, and a binary organic Rankine cycle generator that utilizes low-temperature heat sources, discharged from factories, can help mitigate climate change by further unlocking CO_2 neutral energy sources. The refrigerants that are used for the systems above need low pressure and high critical temperature compared to the refrigerants currently used in the refrigeration and air conditioning equipment. For preventing global warming, the refrigerant conversion from hydrofluorocarbons (HFCs) to new synthetic hydrofluoroolefines (HFO) and hydrochlorofluoroolefin (HCFO) is happening. With the development of low-global warming potential (GWP) and natural refrigerants, several studies are being conducted on the feasibility of replacing drop-in refrigerants with HFC refrigerants. The HFO refrigerants, R1336mzz(Z) and R1336mzz(E), as well as HCFO refrigerants, R1224yd(Z) and R1233zd(E), have similar thermophysical properties to conventional HFC refrigerants, which is advised to substitute R245fa.

In this study, the flow boiling heat transfer of low-pressure refrigerants including R1224yd(Z), R1233zd(E), R1336mzz(E), and R1336mzz(Z) inside a horizontal smooth copper tube with an inner diameter of 8.4 mm were experimentally investigated. In addition, the effects of the mass velocity and vapor quality on the flow boiling heat transfer were clarified. The results were compared with the results of previous studies. On that basis, a new correlation for flow boiling heat transfer considering the flow pattern and post-dryout flow was developed.

2. EXPERIMENTAL SETUP AND DATA REDUCTION

2.1 Experimental setup

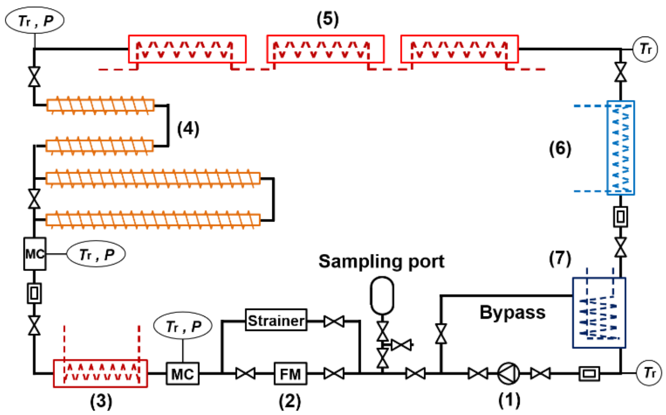

(1) Gear pump
(2) Coriolis-type mass flow meter
(3) Water preheater
(4) Electric preheater
(5) Test section
(6) After-cooler
(7) Receiver tank

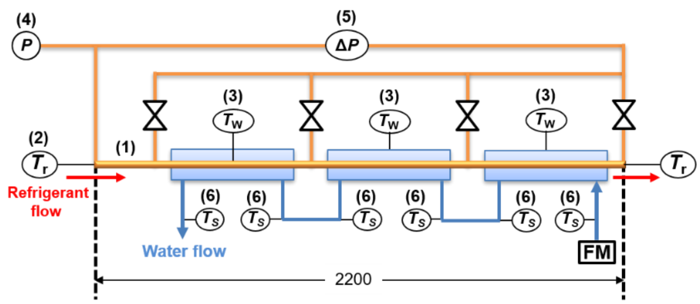

(1) Test tube
(2) Sheathed K-type thermocouple
(3) T-type thermocouple
(4) Absolute pressure transducer
(5) Differential pressure transducer
(6) Pt-resistance thermometer

Figure 2: Detailed view of the test section

Figure 1 shows a schematic of the experimental setup used in this study. The refrigerant loop comprises a gear pump (1), Coriolis-type mass flow meter (2), water preheater (3), electric preheater (4), test section (including three subsections) (5), cooler (6), and receiver tank (7). A subcooled refrigerant, pumped by the gear pump, was adjusted to a predetermined vapor quality at the counter-flow-type water preheater and electric preheater, followed by its flow into the test section. The refrigerant mass flow rate was controlled by the rotational speed of the pump. The aftercooler was supplied with the cooling or heating water mainly to adjust the refrigerant pressure. The flow rate of the test refrigerant was measured using a Coriolis-type mass flow meter.

Figure 2 shows a detailed view of the test section. The test section was a counter-flow-type double-pipe heat exchanger at a length of 2.2 m. In this section, the refrigerant flew through the inner test tube, whilst the heat source water flew through the outer annulus channel, which surrounded the inner tube. The test tube comprises three subsections with an effective heating length of 557 mm. The bulk temperatures of the refrigerant at the inlet and outlet of the test section were measured by sheathed K-type thermocouples with a measurement accuracy of ±0.05 K. The outer tube wall temperature was measured using T-type thermocouples that were attached to the top, bottom, and sides of the exterior wall at the test tube center. The heat source water temperature was measured by Pt-resistance thermometers that were inserted in the mixing chambers at the inlet and outlet of each subsection. An absolute pressure transducer with an accuracy of ±0.75 kPa measured the refrigerant pressure at the inlet of the test section, while two differential pressure transducers with different full scales of 10 and 50 kPa measured the pressure drop between the inlet and outlet of each subsection.

2.2 Data reduction

The heat flux q based on the actual heat transfer area for each subsection is given by

$$q = Q_{\mathrm{S}} / (\pi d_{\mathrm{i}} L) = \left(W_{\mathrm{s}} c_{ps} \Delta T_{\mathrm{s}} - Q_{\mathrm{loss}} \right) / (\pi d_{\mathrm{i}} L) \tag{1}$$

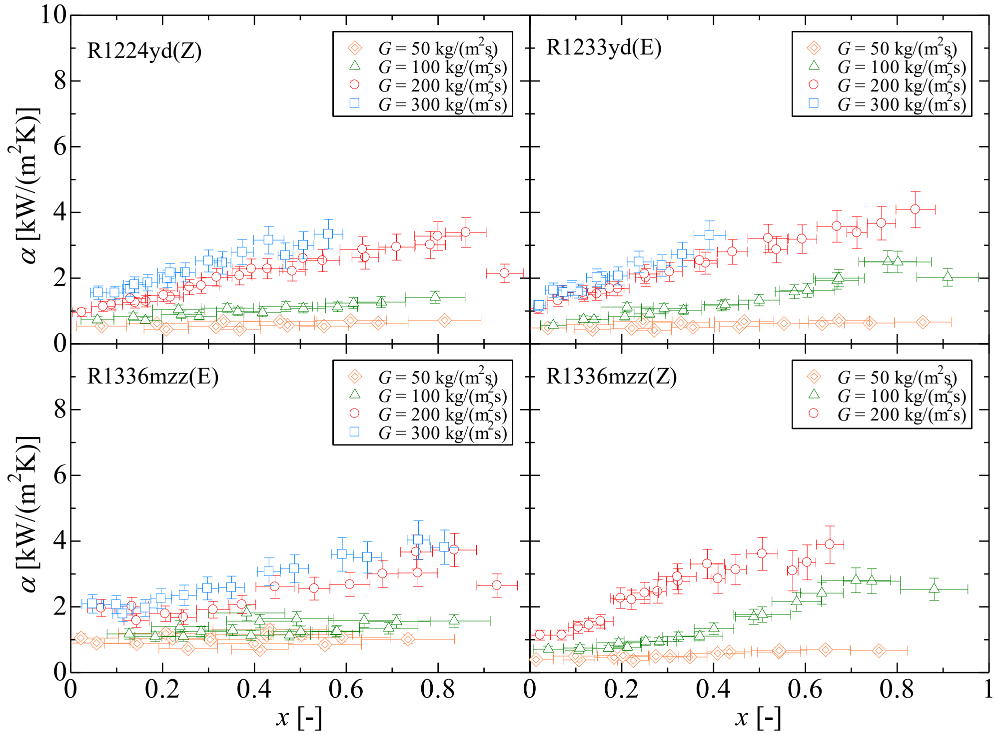

Figure 3: The relationship between boiling HTCs and vapor quality

where W_s and c_{ps} are the mass flow rate and specific heat capacity of the heat source water, respectively, and ΔT_s is the temperature difference of the heat source water between the inlet and outlet of each subsection. The sectional boiling heat transfer coefficient (HTC) α is defined by

$$\alpha = q/\left(T_{wi} - T_r\right) \tag{2}$$

T_r is the refrigerant temperature, which is calculated using the inlet and outlet temperatures at the test section by interpolation for each subsection, and T_{wi} is the inner wall temperature, which can be calculated using Fourier's law and measured outer wall temperature T_{wo}:

$$T_{wi} = T_{wo} - Q_s/\left(2\pi \cdot \lambda \cdot L\right)\ln\left(d_o/d_i\right) \tag{3}$$

3. RESULTS AND DISCUSSION

3.1 HTC of flow boiling

Figure 3 shows the measured HTCs of R1224yd(Z), R1233zd(E), R1336mzz(E), and R1336mzz(Z) with vertical bars indicating the combined measurement uncertainty at mass velocities of 50–300 kgm^{-2}s^{-1} and a saturation temperature of 40 °C. HTC increases with the vapor quality for the mass velocity range of 100–300 kgm^{-2}s^{-1} due to the increment in the forced convection heat transfer and the reduction of thermal resistance. A decline within the vapor quality range of 0.9–1 was identified because of the dryout phenomenon. For all the test refrigerants, the HTC increased at the mass velocities from 100 to 200 kgm^{-2}s^{-1}, owing to the flow pattern transition from the stratified flow to the annular flow.

3.2 Comparison of HTC among the refrigerants

Figure 4 shows the comparison of HTCs among R245fa, R1224yd(Z), R1233zd(E), R1336mzz(E), and R1336mzz(Z) at mass velocities of 50−300 kgm^{-2}s^{-1}. It is observed that the HTC curves of low-GWP refrigerants are nearly identical to those of R245fa. The HTC of R1336mzz(Z) is maximally 2.4 times higher than those of the other refrigerants, particularly at the mass velocity of 100 kgm^{-2}s^{-1} and vapor qualities more than 0.6, mainly due to the 0.4–0.7 times lower vapor density of R1336mzz(Z) than those of the other refrigerants.

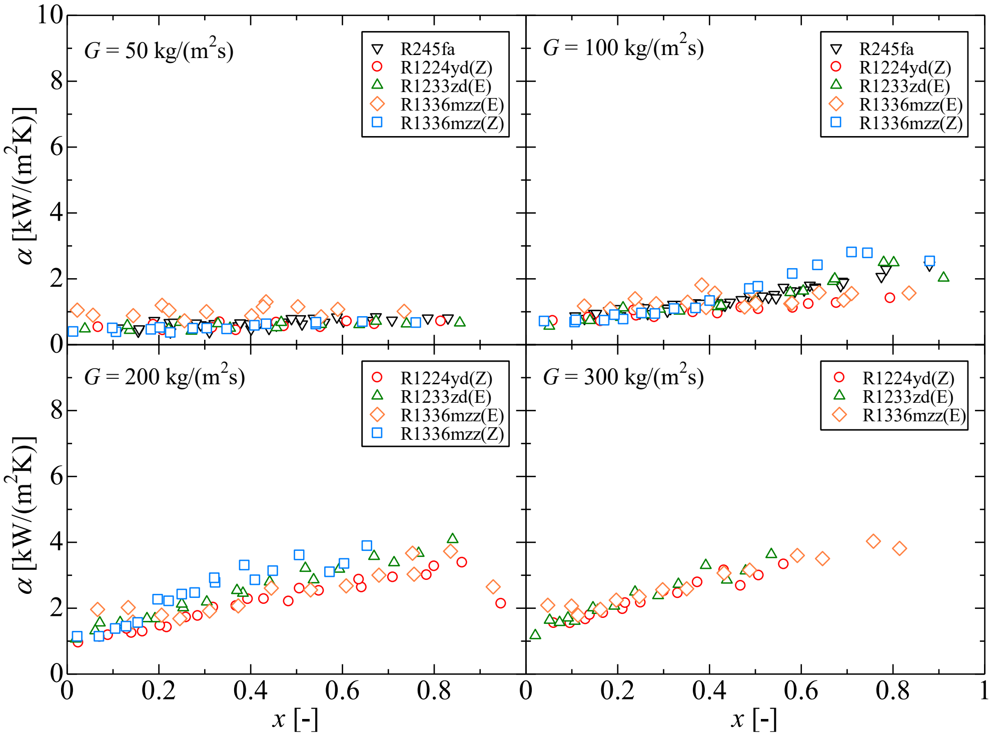

Figure 4: HTCs of R245fa, R1224yd(Z), R1233zd(E), R1336mzz(E), and R1336mzz(Z) inside the smooth copper tube

4. A NEW HEAT TRANSFER CORRELATION

4.1 Discriminant of flow patterns

In this study, the boiling flow heat transfer model is divided into three flow patterns: annular flow, stratified flow, and post-dryout flow. Therefore, it is necessary to differentiate the transition between the annular and stratified flow. The flow patterns can be determined by the wettability separation angles introduced by Mori et al. (2003), using the following equations. In addition, to avoid the iteration, the geometrical expression for the wettability separation angle φ_0 can be calculated using an approximate expression and evaluated in terms of void fraction ξ. (Biberg 1999)

$$\frac{\varphi_{\mathrm{s}}}{\varphi_0} = 1 + 0.75\left[\left(\frac{x}{1-x}\right)\left(\frac{\rho_{\mathrm{L}}}{\rho_{\mathrm{V}}}\right)^{0.5}\right]^{n} \exp\left[1.06 - 23.8\left(\frac{\rho_{\mathrm{V}}}{\rho_{\mathrm{L}}}\right)\right] \tag{4}$$

$$n = 0.26\left[\frac{G^2}{g d_{\mathrm{i}} \rho_{\mathrm{V}}\left(\rho_{\mathrm{L}} - \rho_{\mathrm{V}}\right)}\right]^{0.42}\left(\frac{q}{G \Delta h_{\mathrm{LV}}} \times 10^4\right)^{-0.16} \tag{5}$$

$$\varphi_0 = \pi(1-\xi) + \left(\frac{3}{2}\pi\right)^{\frac{1}{3}}\left[-(1-2\xi) + (1-\xi)^{\frac{1}{3}} - \xi^{\frac{1}{3}}\right] + \frac{1}{200}\xi(1-\xi)(1-2\xi)\left\{1 + 4\left[\xi^2 + (1-\xi)^2\right]\right\} \tag{6}$$

$$\xi = \left[1 + \left(\frac{1-x}{x}\right)\left(\frac{\rho_{\mathrm{V}}}{\rho_{\mathrm{L}}}\right)\right]^{-1} \tag{7}$$

where, φ_{s}, referred to as the actual wettability separation angle, is the angle from the bottom of the tube to the boundary between the wet and dry parts on the circumference. φ_0 is the wettability separation angle, assuming that the gas slip inside the tube is 1, and the gas-liquid interface is flat and horizontal as described in Figure 5. Mori et al. (2003) classified stratified flow patterns into annular flow when $\varphi_{\mathrm{s}} > 0.9\pi$.

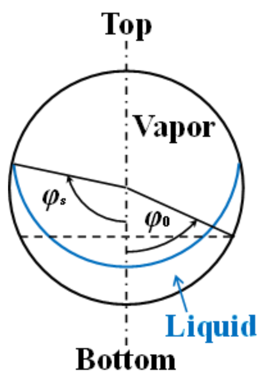

Figure 5: Definition of wettability separation angles

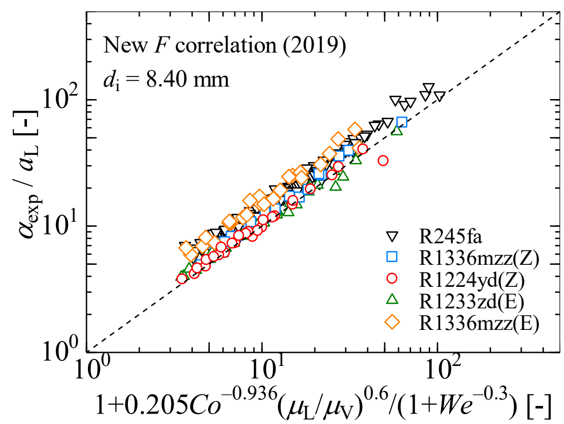

Figure 6: The relationship between $\alpha_{\mathrm{exp}} / \alpha_{\mathrm{L}}$ and F

4.2 The proposed model for annular flow

In this study, a modified Chen correlation model was proposed by fitting the measured flow boiling HTCs. The annular flow boiling HTC consists of convective boiling heat transfer α_{cv} and nucleate boiling heat transfer α_{nb}.

$$\alpha = \alpha_{\mathrm{cv}} + \alpha_{\mathrm{nb}} = F\alpha_{\mathrm{L}} + S\alpha_{\mathrm{pb}} \tag{8}$$

where, F is the Reynolds number factor, α_{L} is the liquid-phase HTC, S is the suppression of nucleate boiling, and α_{pb} is the pool boiling HTC.

4.2.1 Convective boiling heat transfer α_{cv}:
The boiling forced convection heat transfer based on the Dittus-Boelter correlation is expressed as follows:

$$\alpha_{\mathrm{L}} = 0.023\frac{\lambda_{\mathrm{L}}}{d_{\mathrm{i}}}\left[\frac{G(1-x)d_{\mathrm{i}}}{\mu_{\mathrm{L}}}\right]^{0.8} Pr_{\mathrm{L}}^{0.4} \tag{9}$$

For the convective boiling heat transfer, the vapor shear force is dominant. The experimental results showed larger values than those of the conventional refrigerants, such as R134a and R32, which was because the vapor densities of low-pressure refrigerants were significantly lower, and the liquid viscosities of low-pressure refrigerants were larger than the conventional refrigerants were. Therefore, the effect of viscosity on the fluid flow conditions is expressed by the convective numbers, Co and $(\mu_{\mathrm{L}}/\mu_{\mathrm{V}})$, instead of the Lockhart-Martinelli parameter, χ_{tt}. Furthermore, Saitoh et al. (2009) indicated that when the tube diameter changed, the surface tension and buoyancy interactively affected the two-phase flow. Consequently, the effect of tube diameter on the fluid flow conditions was expressed by the Weber number, We_{V}. The Reynolds number factor F is expressed as follows:

$$F = 1 + 0.205 \times Co^{-0.94}\left(\frac{\mu_{\mathrm{L}}}{\mu_{\mathrm{V}}}\right)^{0.6}\frac{1}{1+We_{\mathrm{V}}^{-0.3}} \tag{10}$$

$$Co = \left(\frac{1-x}{x}\right)^{0.8}\left(\frac{\rho_{\mathrm{V}}}{\rho_{\mathrm{L}}}\right)^{0.5} \tag{11}$$

$$We_{\mathrm{V}} = G^2x^2d_{\mathrm{i}}/(\sigma\rho_{\mathrm{V}}) \tag{12}$$

Figure 6 shows the ratio between the experimental value α_{exp} and the liquid single-phase HTC α_{L} with the Reynolds number factor F in the annular flow region, where forced convection is dominant. In Figure 6, the proposed convective heat transfer correlation is aligned with the experimental results.

4.2.2 Nucleate boiling heat transfer α_{nb}:

Jung et al. (2004) proposed a pool boiling heat transfer correlation considering low-pressure refrigerants data as follows:

$$\alpha_{\mathrm{nb}} = 41.4\frac{\lambda_{\mathrm{L}}}{d_b}\left(\frac{q}{\lambda_{\mathrm{L}}}\frac{d_b}{T_{\mathrm{sat}}}\right)^{C}\left(-\log_{10} P_{\mathrm{r}}\right)^{-1.52}\left(1-\frac{\rho_{\mathrm{V}}}{\rho_{\mathrm{L}}}\right)^{0.53} \tag{13}$$

$$C = 0.835\left(1-P_{\mathrm{r}}\right)^{1.33} \tag{14}$$

The suppression factor *S*, defined as the ratio of the effective superheat to the total wall superheat, can be expressed as a function of the local two-phase Reynolds number. The effect of heat flux is represented by the boiling number of nucleate boiling. Therefore, the factor *S* is calculated as follows:

$$S = \frac{1}{1+\left[\frac{G(1-x)d_{\mathrm{i}}}{\mu_{\mathrm{L}}}F^{1.25}\times 10^{-4}\right]^{0.3}\left(\frac{q}{G\Delta h_{\mathrm{LV}}}\times 10^{4}\right)^{-0.3}} \tag{15}$$

4.3 The proposed model for stratified flow

For the stratified flow model, the tube was divided into the upper and lower parts, a portion of the circumference occupied by each part was weighed by the wettability separation angles, calculated by Equations (4–7), and the correlation was expressed as follows:

$$\alpha = \alpha_{\mathrm{wet}} + \alpha_{\mathrm{top}} \tag{16}$$

$$\alpha_{\mathrm{top}} = \left(1-\frac{\varphi_{\mathrm{s}}}{\pi}\right)\alpha_{\mathrm{V}} \tag{17}$$

where α_{V} is the dry-perimeter HTC:

$$\alpha_{\mathrm{V}} = 0.023\frac{\lambda_{\mathrm{V}}}{d_{\mathrm{i}}}\left(\frac{Gxd_{\mathrm{i}}}{\mu_{\mathrm{V}}}\right)^{0.8} Pr_{\mathrm{V}}^{0.4} \tag{18}$$

The average HTC of the wetted perimeter can be expressed by the wettability separation angles as follows:

$$\alpha_{\mathrm{wet}} = \frac{\varphi_{\mathrm{s}}}{\pi}\left(F\alpha_{\mathrm{L}} + S\alpha_{\mathrm{pb}}\right) \tag{19}$$

The prediction method proposed for the stratified flow regime takes into account the effect of circumferential heat conduction in the tube wall. For the nucleate boiling heat transfer, α_{nb} is given by the same correlations; while the suppression of nucleate boiling *S*, is given by a slightly different equation:

$$S = \frac{1}{1+\frac{\varphi_{\mathrm{s}}}{\pi}\left[\frac{G(1-x)d_{\mathrm{i}}}{\mu_{\mathrm{L}}}F^{1.25}\times 10^{-4}\right]^{0.3}\left(\frac{q_{\mathrm{wet}}}{G\Delta h_{\mathrm{LV}}}\times 10^{4}\right)^{-0.3}} \tag{20}$$

where q_{wet} is the average heat flux of the wetted perimeter.

$$q_{\mathrm{wet}} = \left(\pi/\varphi_{\mathrm{s}}\right)q \tag{21}$$

4.4 The proposed model for post-dryout flow

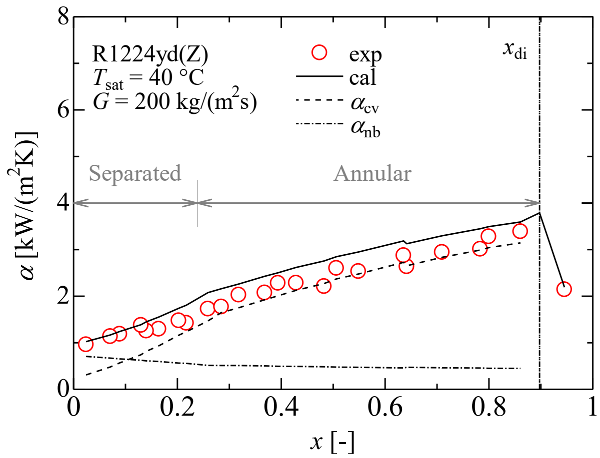

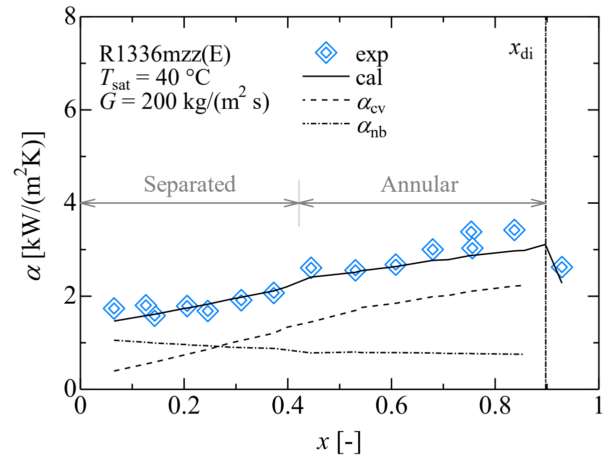

Figure 7: The relationship between the calculated and experimental HTCs and vapor quality

Mori et al. (2000) defined a dryout inception x_{di} and a dryout completion x_{de} using three characteristic regimes: S1, S2, and S3. Wojtan et al. (2005) proposed a modified dryout inception based on Mori's S2 correlation. In this study, our experimental data best agreed with Wojtan's correlation. Therefore, vapor quality at the occurrence of dryout in a nnular flow was predicted as follows:

$$x_{di} = 0.58\exp\left[0.52 - 0.235 We_{V}^{0.17} Fr_{V}^{0.37} \left(\frac{\rho_V}{\rho_L}\right)^{0.25} P_r^{0.7}\right] \tag{22}$$

$$Fr_V = \frac{G^2}{\rho_V\left(\rho_L - \rho_V\right) g d_i} \tag{23}$$

Under low heat flux conditions, the correlation of HTC of dryout flow can be calculated using the following simple linear interpolating equation:

$$\alpha_{dryout} = \alpha_{x_{di}} - \frac{x - x_{di}}{1 - x_{di}}\left(\alpha_{x_{di}} - \alpha_V\right) \tag{24}$$

Table 1: Prediction deviations of each correlation

Correlation	Year	N = 692			
		MAD [%]	MD [%]	R20 [%]	R30 [%]
Chen	1966	68.8	40.1	19.7	31.5
Gungor and Winterton	1986	28.6	−3.0	36.7	55.1
Gungor and Winterton	1987	29.9	−3.4	34.4	53.6
Kandlikar	1987	29.8	0.7	34.7	52.0
Jung et al.	1989	32.1	−11.6	29.1	39.7
Liu and Winterton	1991	37.9	−31.7	26.2	36.0
Takamatsu et al.	1992	39.5	30.6	37.7	59.1
Mori et al.	1999	17.5	−8.1	58.7	71.7
Yu et al.	1999	34.2	10.0	31.8	44.5
Choi et al.	2000	131.0	129.4	21.4	30.4
Saitoh et al.	2007	35.7	−0.3	29.2	42.2
Sun and Mishima	2009	39.3	−24.7	31.8	39.2
Present	2020	17.2	−1.0	63.2	83.5

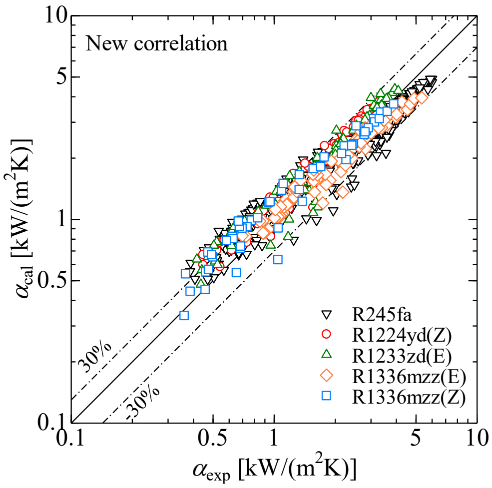

Figure 8: Comparison between the experimental and calculated values using the proposed correlation

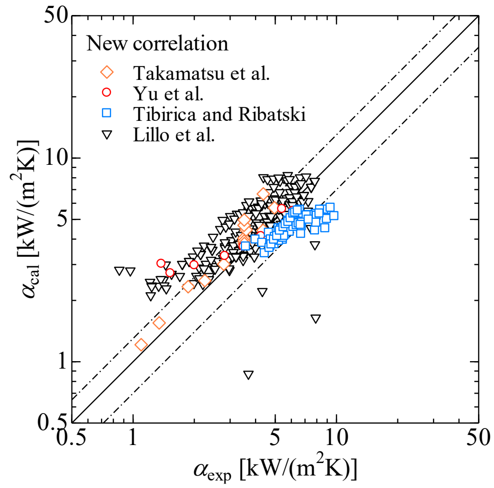

Figure 9: Comparison between the calculated and experimental values of the other studies

5. VERIFICATION OF THE PROPOSED CORRELATION

Figure 7 along with the equations in Section 4 verify the reasonable performance of the proposed prediction model for the tested R1224yd(Z) and R1336mzz(E) at a saturation temperature of 40 °C. As shown in Figure 7, the overlap between the solid line and blue rhombuses confirms an excellent agreement between the proposed prediction model and the experimental data. Figure 7 verifies the sharp decrease of vapor quality from 0.9 to 1, and the occurrence of post-dryout flow. In addition, Figure 8 compares the results of HTC and experimental data for low-pressure refrigerants. According to Figure 8, the proposed correlation predicted HTCs for both the annular and stratified flows acceptably.

Furthermore, The measured HTC were compared with the predicted values using the correlations introduced in other studies: Chen (1966), Gungor and Winterton (1986, 1987), Kandlikar (1987), Jung et al. (1989), Liu and Winterton (1991), Takamatsu et al. (1992), Mori et al. (1999), Yu et al. (1999), Choi et al. (2000), Saitoh et al. (2007), and Sun and Mishima (2009). Table 1 lists the deviations between the experimental and predicted values. MAD and MD in Table 1 denote the mean absolute deviation and mean deviation, respectively. MD and MAD are calculated as follows:

$$\mathrm{MD} = \frac{1}{n}\sum^{n}\left(\frac{\alpha_{\mathrm{cal}} - \alpha_{\mathrm{exp}}}{\alpha_{\mathrm{exp}}}\right) \tag{25}$$

$$\mathrm{MAD} = \frac{1}{n}\sum^{n}\left|\frac{\alpha_{\mathrm{cal}} - \alpha_{\mathrm{exp}}}{\alpha_{\mathrm{exp}}}\right| \tag{26}$$

R20 and R30 denote the ratio of the number of data points within ±20 and ±30 % deviation to the total number of measured data points, respectively. According to Table 1, the existing correlations developed from Chen's model acceptably predicted the data with a mean deviation of approximately ±30 %. The correlation proposed by Mori et al. (2003), which is based on the wettability separation angles to distinguish between the stratified and annular flows,

Table 2: The experimental conditions and number of data in the previous studies on the low-pressure refrigerants

Source	Fluid	Saturation pressure, kPa (Temperature, °C)	d_i mm	G kgm^{-2}s^{-1}	q kWm^{-2}	N
Takamatsu et al. (1992)	R114	450-460 (50.3-51.1)	7.9	299-301	4.5-38.6	15
Yu et al. (1999)	R123	260 (56.7)	8.4	301	12.5-46.1	8
Tibirica and Ribtski (2010)	R245fa	190-288 (31)	2.3	200-700	10-25	70
Lillo et al. (2019)	R1233zd(E)	131-673 (24.9-65)	6	150-300	2.45-40.1	259

reasonably agreed with our experimental results, where R30 was higher than 71 %.

In this comparison, the proposed correlation agreed moderately well with the HTC experimental data obtained from different low-pressure refrigerants, where the mean deviation and R30 of the modified correlation were 1.0 % and 83.5 %, respectively.

Figure 9 compares the correlations of the HTC and the measured data on the low-pressure refrigerants conducted by Takamatsu et al. (1992), Yu et al. (1999), Tibirica and Ribtski (2010), and Lillo et al. (2019). The experimental conditions and number of data are listed in Table 2. Figure 9 shows that the proposed correlation provided satisfactory predictions of the measured data approximately with a variation rate of ±30 %.

6. CONCLUSIONS

The characteristics of the flow boiling heat transfer of low-pressure refrigerants R245fa, R1224yd(Z), R1233zd(E), R1336mzz(Z), and R1336mzz(E) were studies inside a horizontal smooth tube. A new flow boiling heat transfer model for low-pressure refrigerants inside horizontal smooth tubes was proposed. The conclusions were as follows:

- HTC of R1336mzz(Z) was higher than those of the other refrigerants, mainly due to the higher vapor density.
- Based on the correlations introduced by Mori et al. (1999), a modified heat transfer correlation was developed based on a wettability separation angle to differentiate the stratified and annular flows. In addition, the HTC after the onset of dryout vapor quality was investigated. The proposed prediction model and the experimental HTC exhibited an excellent agreement. The MD and R30 of the modified correlation were 1.0 % and 83.5 %, respectively.

NOMENCLATURE

Co	convective number	(–)
c_p	constant pressure specific heat	($J\ kg^{-1}\ K^{-1}$)
d	diameter	(m)
F	Reynolds number factor	(–)
Fr	Froude number	(–)
G	mass flow rate	($kg\ m^{-2}\ s^{-1}$)
L	effective heating length	(m)
Pr	Prandtl number	(–)
q	heat flux	($W\ m^{-2}$)
Q	heat flow	(W)
S	suppression factor	(–)
T	temperature	(K or °C)
W	mass flow	($kg\ s^{-1}$)
We	Weber number	(–)
x	vapor quality	(–)
α	HTC	($W\ m^{-2}\ K^{-1}$)
Δh_{LV}	latent energy	($J\ kg^{-1}$)
ξ	void rate	(–)
φ_s	wettability separation angle	(rad)
λ	thermal conductivity	($W\ m^{-1}\ K^{-1}$)
μ	viscosity	(Pa s)
ρ	density	($kg\ m^{-3}$)
σ	surface tension	($N\ m^{-1}$)

Subscript

cal	calculate
crit	critical point
cv	convective
di	dryout inception
exp	experiment
i	inner
L	liquid
nb	nucleate boiling
pb	pool boiling
r	refrigerant
s	source water
sat	saturated
V	vaper
w	wall

REFERENCES

Biberg, D.(1999). An Explicit Approximation for the Wetted Angle in Two−phase Stratified Pipe Flow. *The Canadian Journal of Chemical Engineering*, *77*, 1221–1224.

Chen, J. C. (1966). Correlation for Boiling Heat Transfer to Saturated Fluids in Convective Flow. *Industrial & Engineering Chemistry Process Design and Development*, *5*(3), 322–329.

Choi, T. Y., Kim, Y. J., Kim, M. S., & Ro, S. T. (2000). Evaporation Heat Transfer of R–32, R–134a, R–32/134a, and R–32/125/134a inside a Horizontal Smooth Tube. *International Journal of Heat and Mass Transfer*, *43*(19), 3651–

3660.
Gungor, K. E., & Winterton, H. S. (1986). A General Correlation for Flow Boiling in Tubes and Annuli. *International Journal of Heat and Mass Transfer*, *29*(3), 351–353.
Gungor, K. E., & Winterton H. S. (1987). Simplified general correlation for saturated flow boiling and comparisons of correlations with data. *Chemical Engineering Journal*, *65*, 148–156.
Jung, D., Lee, H., Bae D., & Oho, S. (2004). Nucleate Boiling Heat Transfer Coefficients of Flammable Refrigerants. *International Journal of Refrigeration*, *27*, 409–414.
Jung, D. S., McLinden, M., Radermacher, R., & Didion, D. (1989). A Study of Flow Boiling Heat Transfer with Refrigerant Mixtures. *International Journal of Heat and Mass Transfer*, *32*(9), 1751–1764.
Kandlikar, S. G. (1987). A General Correlation for Saturated Two−phase Flow Boiling Heat Transfer inside Horizontal and Vertical Tubes. *J. HTD*, *85*, 9–19.
Kedzierski, A. M., & Lin L. (2019). Pool Boiling of HFO−1336mzz(Z) on a Reentrant Cavity Surface. *International Journal of Refrigeration*, *104*, 476–483.
Lemmon, E. W., Huber, M. L., & McLinden, M. O. (2018). Reference Fluid Thermodynamic and Transport Properties–REFPROP Ver. 10. National Institute of Standards and Technology, Gaithersburg.
Lillo, G., Mastrullo, R., Mauro, A.W., & Viscito, L. (2019). Flow Boiling of R1233zd(E) in A Horizontal Tube: Experiments, Assessment and Correlation for Asymmetric Annular Flow. *International Journal of Heat and Mass Transfer*, *129*, 547–561.
Liu, Z., & Winterton R.H.S. (1991). A general correlation for saturated and subcooled flow boiling in tubes and annuli based on a nucleate pool boiling equation. *International Journal of Heat and Mass Transfer*, *34*(11), 2759–2766.
Mori, H., Yoshida, S., Hong, H., & Matsunaga, T. (1994). Prediction of Heat Transfer Coefficient for Refrigerants Flowing in Horizontal Evaporator Tubes. *Transactions of the Japan Society of Refrigerating and Air Conditioning Engineers*, *11*(1), 67−78. (in Japanese)
Mori, H., Yoshida, S., Kakimoto, Y., & Ohishi. K. (1999). Reform of the Correlation for the Prediction of Heat Transfer Coefficient for Refrigerants Flowing in Horizontal Evaporator Tubes. *Transactions of the Japan Society of Refrigerating and Air Conditioning Engineers*, *16*(2), 177−187. (in Japanese)
Mori, H., Yoshida, S., Kakimoto, Y., Ohishi, K., & Fukuda, K. (2000). Post-dryout heat transfer to a refrigerant flowing in Horizontal evaporator tubes, *Transactions of the Japan Society of Refrigerating and Air Conditioning Engineers*, *17*(4), 521−528. (in Japanese)
Thermal Sciences Conference, 2000, pp. 839–844.
Saitoh S., Daiguji H., & Hihara E. (2007). Correlation for Boiling Heat Transfer of R−134a in Horizontal Tubes Including Effect of Tube Diameter. *International Journal of Heat and Mass Transfer*, *50*, 5215–5225.
Sun, L., & Mishima, K. (2009). An Evaluation of Prediction Methods for Saturated Flow Boiling Heat Transfer in Mini–Channels. *International Journal of Heat and Mass Transfer*, *52*(23–24), 5323−5329.
Takamatsu, H., Momoki, S., & Fujii, T. (1992). A Correlation for Forced Convection Boiling Heat Transfer of Single-Component Refrigerants in a Horizontal Smooth Tube. *Transactions of the Japan Society of Mechanical Engineers* (B), *58*(550), 1875–1882. (in Japanese)
Tibiriçá, C.B., & Ribatski, G. (2010). Flow Boiling Heat Transfer of R134a and R245fa in a 2.3 mm Tube. *International Journal of Heat and Mass Transfer*, *53*(11–12), 2459–2468.
Wojtan L., Ursenbacher T.., & Thome R. J. (2005). Investigation of Flow Boiling in Horizontal Tubes: Part I − A New Diabatic Two−phase Flow Pattern Map. *International Journal of Heat and Mass Transfer*, *48*, 2955–2969.
Yu, J., Momoki, S., & Koyama, S. (1999). Experimental Study of Surface Effect on Flow Boiling Heat Transfer in Horizontal Smooth Tubes. *International Journal of Heat and Mass Transfer*, *42*(10), 1909−1918.

ACKNOWLEDGEMENT

This study was supported by the Mechanical Engineering Laboratory of Kobe Steel, LTD. We would like to express our gratitude here.